

Dicationic State of Dithiadiazafulvalene within a TCNQ Charge-Transfer Complex: Generation and Characterization

N. Bellec,[†] D. Lorcy,^{*,†} K. Boubekeur,^{*,‡} R. Carlier,[†] A. Tallec,[†] Sz. Los,[§] W. Pukacki,^{||} M. Trybula,^{*,§} L. Piekara-Sady,^{*,§} and A. Robert[†]

Synthèse et Electrosynthèse Organiques, UMR CNRS 6510, Université de Rennes 1, campus de Beaulieu, 35042 Rennes Cedex, France; Laboratoire de Chimie des Solides, UMR CNRS 6502, Institut des Matériaux de Nantes, 2 rue de la Houssinière, 44072 Nantes, France; Institute of Molecular Physics, Polish Academy of Sciences, Poznań, PL-60-179, Poland; and Department of Physics, Agricultural University, Poznań, Poland

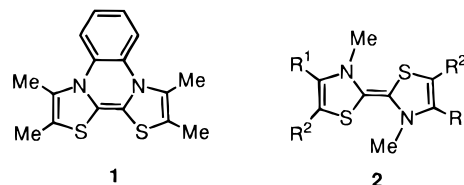
Received April 21, 1999. Revised Manuscript Received August 4, 1999

Dithiadiazafulvalenes (DTDAF) can be formed either chemically or electrochemically. Electrochemical investigations have been carried out on 2-ethylthio-1,3-thiazolium salts to determine the redox behavior of dithiadiazafulvalenes formed by cathodic coupling. Using an in situ method, the donor has been trapped in the medium and a crystalline charge-transfer salt with TCNQ has been isolated. The crystal structure and magnetic susceptibility data of this 1:3 complex established that the DTADF is in the dicationic state.

Introduction

Tetrathiafulvalenes (TTF) derivatives have been widely used as components for the formation of organic materials.¹ Dithiadiazafulvalenes (DTDAF), their aza analogues, where two sulfur atoms have been replaced by nitrogen have attracted attention in this field, but few examples of charge-transfer salts have been reported.^{2–6} This is due to the fact that DTDAFs, compared to TTFs, present extremely high electron-donating properties and therefore are very difficult to handle for the synthesis of such molecular materials.^{6–8} Nevertheless Cava et al. reported charge-transfer complexes showing appreciable conductivity between DTDAF, stabilized by electron-withdrawing substituents, and tetracyanoquinodimethane (TCNQ).⁵ These results confirmed the potential of these donors, but so far no structural characterization of the TCNQ complexes has been given. To prepare new charge-transfer salts, we developed an original strategy which consists of forming the DTDAF donor core and trapping it with an in situ method by adding the acceptor directly into the medium. Using this in situ method, we recently prepared quasi-planar

DTDAF **1**, by *intramolecular* coupling of N,N'-bridged bithiazoline selone, and isolated the corresponding *radical cation*.⁶ Along these lines, we have now examined a similar approach but involving in this case an *intermolecular* coupling of thiazoline selone to synthesize the less hindered donor DTDAF **2**, and form the corresponding *dication*. In this article we report the



synthesis of various substituted DTDAF **2** derivatives and a dicationic salt of the hexamethyldithiadiazafulvalene. This latter compound, named **2a**·(TCNQ)₃ is fully characterized by an X-ray structure determination and EPR spectroscopy carried out on single crystals. These studies corroborate the dicationic state of the donor in this salt.

Results and Discussion

For the syntheses of compounds **2**, we used the chemical pathway described in Scheme 1. Treatment of dithiocarbamate salt **3** with α -halogenated ketones, followed by cyclization and dehydration in the presence of sulfuric acid yields the thiazolinethiones **4**.⁹ As previously observed, **4** needed to be converted into the thiazoline selone **6** to undergo intermolecular coupling with trivalent phosphorus derivatives.^{5,6}

The synthesis of **2** can also be performed electrochemically. We recently reported the cathodic coupling of

[†] Université de Rennes.

[‡] Institut des Matériaux de Nantes.

[§] Polish Academy of Sciences.

^{||} Agricultural University.

(1) Yamada, J.; Nishikawa, H.; Kikuchi, K. *J. Mater. Chem.* **1999**, 9, 617.

(2) Wheland, R. C.; Gillson, J. L. *J. Am. Chem. Soc.* **1976**, 98, 3916.

(3) Yamashita, Y.; Susuki, T.; Saito, G.; Mukai, T. *Chem. Lett.* **1985**, 1759.

(4) Bssaibis, M.; Robert, A.; Le Maguerès, P.; Ouahab, L.; Carlier, R.; Tallec, A. *J. Chem. Soc., Chem. Commun.* **1993**, 601.

(5) Tormos, G. V.; Bakker, M. G.; Wang, P.; Lakshmikantham, M. V.; Cava, M. P.; Metzger, R. M. *J. Am. Chem. Soc.* **1995**, 117, 8528.

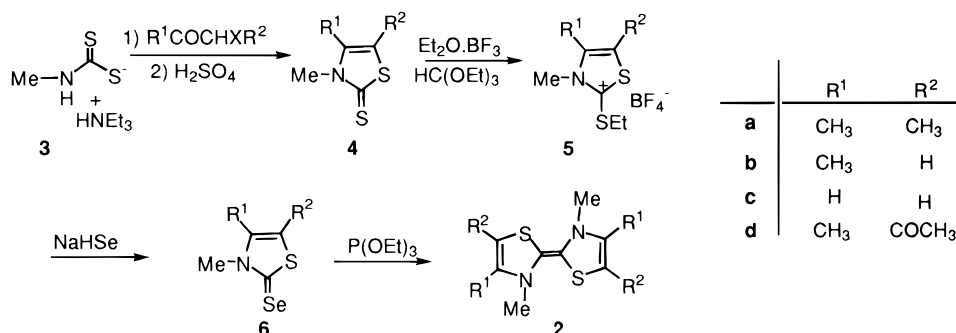
(6) Bellec, N.; Lorcy, D.; Robert, A.; Carlier, R.; Tallec, A.; Rimbaud, C.; Ouahab, L.; Clerac, R.; Delhaes, P. *Adv. Mater.* **1997**, 9(13), 1052.

(7) Bordwell, F. G.; Satish, A. V. *J. Am. Chem. Soc.* **1991**, 113, 985.

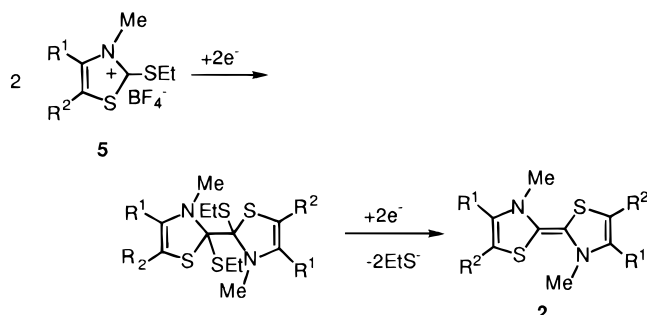
(8) Gouille, V.; Chirayil, S.; Thummel, R. P. *Tetrahedron Lett.* **1990**, 31, 1539.

(9) Humphlett, W. J.; Lamon, R. W. *J. Org. Chem.* **1964**, 29, 2146.

Scheme 1



Scheme 2

Table 1. Cyclic Voltammetry for **1** and **2** Obtained after Electroreduction of Thiazolium Salt^a

	R ¹	R ²	<i>E</i> _{pa} ¹	<i>E</i> _{pa} ²	Δ <i>E</i>
1a ⁶	Me	Me	-0.44	-0.03	0.41
1b ¹⁰	Me	CO ₂ Et	-0.07	0.44	0.51
2d	Me	COMe	-0.28	-0.03	0.25
2e	Me	CO ₂ Et	-0.30	-0.08	0.22
2c ⁸	H	H	-0.54	-0.41	0.13
tetramethyl TTF			0.27	0.65	0.38

^a *E* is in volts vs SCE; supporting electrolyte, 0.1 M Bu₄NPF₆ in CH₃CN; scanning rate, 0.1 V/s.

phenyl-*N,N'*-bridged bis(2-ethylthio-1,3-thiazolium fluoborate) which generates the phenyl-*N,N'*-bridged DTDAF **1**, this electroactive species being detected immediately after the reduction by cyclic voltammetry.¹⁰ Electrochemical investigations performed on the thiazolium salt **5** allowed us to detect dimer formation in the medium (Scheme 2). It appears that the formation of the donor core **2**, by intermolecular coupling of two radical intermediates, is less quantitative than for **1** which results from an intramolecular coupling of a bis radical.¹⁰ Moreover, determination of the oxidation potentials for the electroactive species **2** was possible by electroreduction of the thiazolium salt **5** when withdrawing substituents were linked to the thiazole core. For comparison, oxidation potentials of compounds **1**, **2**, and tetramethyl TTF are collected in Table 1.

As TTF, their sulfur analogues, two main oxidation waves associated with the redox behavior of the DTDAF are observed. All of these DTDAFs exhibit very low oxidation potentials compared to TTF, which proves their excellent donor ability. Another interesting feature, the potential difference observed between the two oxidation states (Δ*E*), is lower for **2** than for *N,N*-phenyl-bridged derivative **1**, indicating that in this case

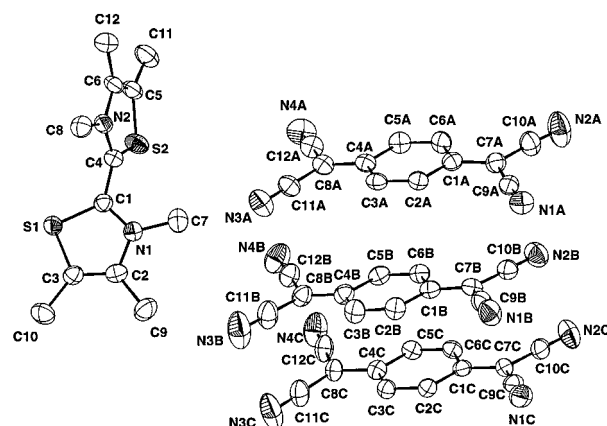


Figure 1. Asymmetric unit of the complex **2a**·(TCNQ)₃ showing the numbering of atoms.

it is easier to reach the dicationic state **2**²⁺. This is even more obvious in the case of the nonsubstituted DTDAF detected after electroreduction of a diquaternary salt of 2,2'-bithiazole by Thummel et al. (Δ*E* = 0.13 V vs SCE).⁸ This peculiarity between dithiadiazafulvalenes substituted on the nitrogen by a methyl group and those bearing an aromatic substituent has also been noticed by Cava et al. for their DTDAFs.⁵

Following our previous work on DTDAF where **1a** was trapped in situ as a radical cation by adding a solution of a polyoxometalate (Bu₄N)₂Mo₆O₁₉ (*E*₀ = -0.32 V vs SCE),⁶ we added to the medium where **2a** is formed a solution of a stronger organic acceptor, TCNQ (*E*₁ = 0.18 V and *E*₂ = -0.37 V vs SCE).¹¹ After the addition of TCNQ, the solution turned from yellow to dark green. Black shiny single crystals appeared after a couple of days at room temperature under an inert atmosphere. The crystal structure determination reveals a stoichiometry of one donor **2a** for three TCNQ (Figure 1).¹² The analysis of the packing shows that the stacks of TCNQ molecules are parallel to *b* and are sandwiched by the donors whose longest axis runs along the same direction (Figure 2). Within the three crystallographically independent TCNQ species A, B, and C, one can observe different overlaps, the TCNQs being offset with a nonuniform intermolecular spacing. The interplanar

(11) Kaplan, M. L.; Haddon, R. C.; Bramwell, F. B.; Wudl, F.; Marshall, J. H. Cowan, D. O.; Gronowitz, S. *J. Phys. Chem.* **1980**, *84*, 427.

(12) STOE IPDS Software, V2.87, STOE&Cie, Darmstadt, 1997. (b) Sheldrick, G. M. *SHELXS-86, Program for Structure Solution*; University of Göttingen: Göttingen, Germany, 1986. (c) G. M. Sheldrick, G. M. *SHELXL-97, Program for Structure Refinement*; University of Göttingen: Göttingen, Germany, 1997.

(10) Bellec, N.; Lorcy, D.; Robert, A.; Carlier, R.; Tallec, A. *J. Electroanal. Chem.* **1999**, *462/2*, 137.

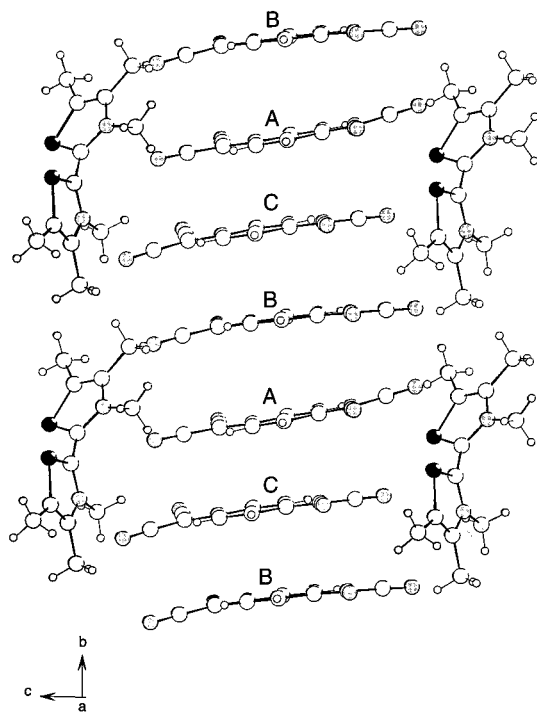


Figure 2. Stack of TCNQ molecules sandwiched by $2a^{2+}$.

separation between A and B and between B and C are respectively 3.486(76) and 3.216(27) Å with a transversal slip (Figure 3 a and b). In contrast a ring-over-bond overlap is observed between pseudo trimers (TCNQs A and C) with a longitudinal slip (Figure 3c) and a shorter interplanar separation (3.126(27) Å).

Within this salt, the donor is not planar (Figure 1), the two thiazole rings are twisted around the C1–C2 bond by an angle of 76°. A large dihedral angle between the thiazolium rings suspected by Thummel et al. during the course of their studies by electronic absorption spectra on various bisthiazolium salt⁸ is unambiguously confirmed here. This result differs strongly from those observed with the BEDT–TTF framework where the cation radical and dication are almost planar.¹³ In contrast, in the neutral donor **2a** described by Arduengo¹⁴ or the neutral BEDT–TTF,¹⁵ distortions from planar geometry are observed. It is worth noting that in the case of DTDAF important conformational modifications between the neutral and the oxidized state of the same donor **2a** occur.

Depending on the oxidation state, modifications of the bond lengths of DTDAF are observed. Upon oxidation, the central double bond is lengthened while C–N and C–S bonds are shortened when compared with the neutral molecule (Table 2). This behavior finds its origin in the nature of the HOMO in **2a**. Actually calculations by a semiempirical method (PM3) show bonding interactions between carbon atoms and antibonding interactions between the heteroatoms (nitrogen or sulfur) and carbon atoms.¹⁶ One can note the close topology of the HOMO's in **2a** and TTF (Figure 4). Likewise, modifica-

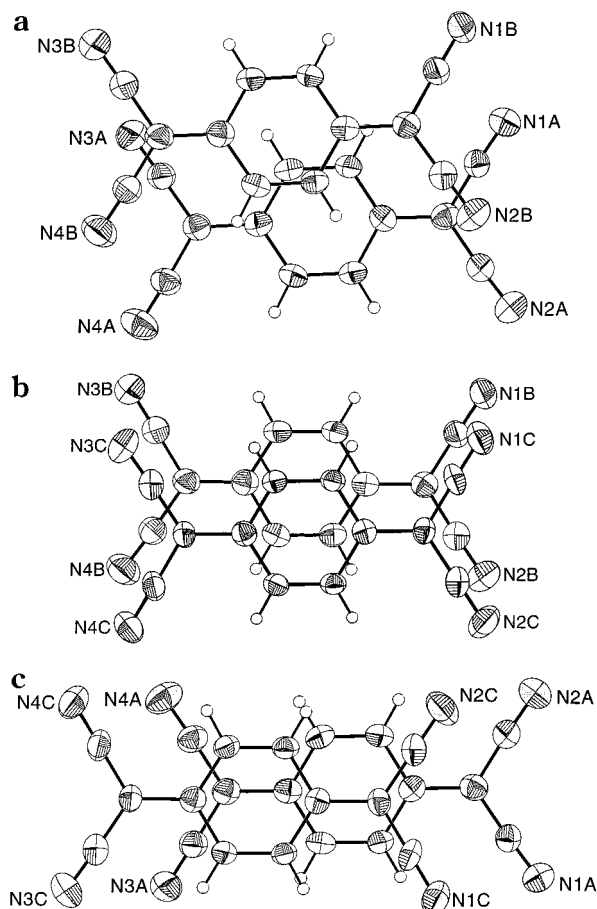


Figure 3. TCNQ molecular overlaps (a) TCNQ A and TCNQ B, (b) TCNQ B and TCNQ C and (c) TCNQ C and TCNQ A.

tions were observed in the TTF skeleton as can be seen for the neutral, cation radical, and dication state of BEDT–TTF in Table 2.

Accordingly, comparison of the bond lengths in the TTF skeleton have often been used for the determination of the oxidation state of donors in charge-transfer salts. The hexamethyl DTDAF **2a** in its TCNQ salt exhibits the longest central C–C bond (1.469(4) Å) in the series of DTDAF. The comparison of this bond length with the central C–C bond observed in N,N'-bridged DTDAF cation radical⁶ favors a dication state for the donor in this DTDAF·(TCNQ)₃ salt. IR and EPR studies carried out on crystals are in agreement with this oxidation state (vide infra).

By using the empirical formula of Kistenmacher which correlates the bond lengths to the formal charge of the TCNQ in various charge-transfer salts,¹⁷ we derived the values of –0.47, –0.92, and –0.77 for the formal charges of TCNQ's A, B, and C, respectively. This is supported by the broad nitrile stretching absorption band at 2197 cm^{–1} in the FTIR spectra of the complex **2a**·(TCNQ)₃ (ν_{CN} = 2227 cm^{–1} for neutral TCNQ, 2183 cm^{–1} for TCNQ^{–1}).¹⁸ The total charge transfer of approximately +2 between **2a** and three TCNQ confirms that the donor is in its dicationic form.

(13) Chou, L. K.; Quijada, M. A.; Cleverger, M. B.; de Oliveira, G. F.; Abboud, K. A.; Tanner, D. B.; Talham, D. R. *Chem. Mater.* **1995**, 7, 530.

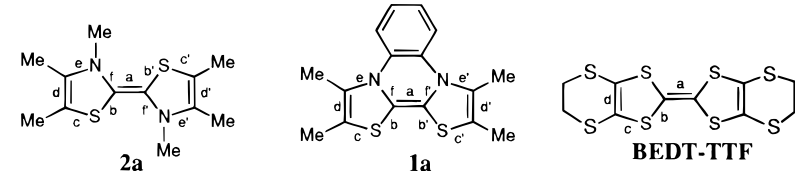
(14) Arduengo, A. J.; Goerlich, J. R.; Marshall, W. J. *Liebigs. Ann. Recueil* **1997**, 365.

(15) Kobayashi, H.; Kobayashi, A.; Sasaki, Y.; Saito, G.; Inokuchi, H. *Bull. Chem. Soc. Jpn.* **1986**, 59, 301.

(16) Stewart, J. P. P. MOPAC Version 6.0. USAF Academy, QCPE 455.

(17) Kistenmacher, T. J.; Emge, T. J.; Bloch, A. N.; Cowan, D. O. *Acta Crystallogr.* **1982**, B38, 1193.

(18) Chappel, J. S.; Bloch, A. N.; Bryden, W. A.; Maxfield, M.; Poehler, T. O.; Cowan, D. O. *J. Am. Chem. Soc.* **1981**, 103, 2442.

Table 2. Bond Lengths (Å) for 2a, 1a⁺, 2a²⁺, and for BEDT-TTF


	2a ^a	1a ^{++b}	2a ²⁺	BEDT-TTF ^c	BEDT-TTF ^{++ d}	BEDT-TTF ^{2+ d}
a	1.341(2)	1.37(1)	1.469(4)	1.312(12)	1.390(7)	1.439(4)
b	1.779(2)	1.691(8)	1.692(3)	1.757(7)	1.721(3)	1.683(3)
b'	1.762(2)	1.698(8)	1.689(3)			
c	1.764(2)	1.758(9)	1.718(3)	1.754(8)	1.738(4)	1.716(3)
c'	1.769(2)	1.740(8)	1.714(3)			
d	1.339(2)	1.31(1)	1.342(4)	1.332(7)	1.365(6)	1.379(5)
d'	1.329(2)	1.33(1)	1.351(5)			
e	1.397(2)	1.42(1)	1.396(4)			
e'	1.432(2)	1.40(1)	1.393(4)			
f	1.438(2)	1.38(1)	1.316(4)			
f'	1.396(2)	1.39(1)	1.337(4)			

^a Reference 14. ^b Reference 6. ^c Reference 15. ^d Reference 13.

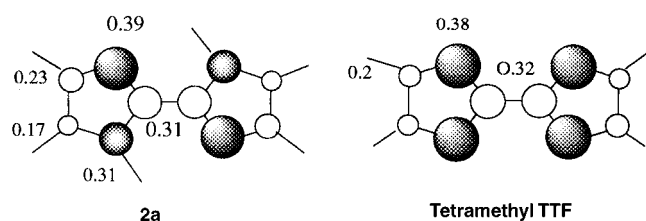


Figure 4. HOMO of 2a (left) and tetramethyl TTF (right).

Table 3. Principal Values and Directional Cosines of the Principal Axes System of g^2 Tensor Relative to the Experimental Axes System a^* , b^* , and c (at room temperature)

axes	directional cosines			g
	a^*	b^*	c	
g_{xx}	-0.329	0.117	-0.937	2.0028
g_{yy}	-0.938	-0.154	0.310	2.0034
g_{zz}	-0.108	0.981	0.160	2.0028

EPR studies were carried out on a single crystal. The EPR signal at room temperature consists of a single Lorentzian line at $g \approx 2$ corresponding to the TCNQ radical anion. Both, the resonance field and the line width depend on the angle between the static magnetic field and the crystallographic axes. Angular dependencies of single-crystal EPR spectra were recorded at room temperature for three mutually perpendicular crystal planes in the reference system a^* , b^* , and c . It has been found that the needle axis of the studied crystal is parallel to the c axis and that the largest face is a (001) plane. The variation of the g factor with the orientation in the magnetic field is described by¹⁹

$$g^2 = g_{aa}^2 \cos^2(\theta_a) + g_{bb}^2 \cos^2(\theta_b) + g_{cc}^2 \cos^2(\theta_c)$$

where g_{ii} is the principal value of g^2 tensor and θ_i is the angle between the principal axis i and the static magnetic field direction. The principal values of g tensor and directional cosines are assembled in Table 3. Because of the very broad signals, the accuracy of g tensor components is quite low. The average of the principal g values equals 2.0030. This value is close to

the g value of TCNQ⁻ in solution $g = 2.0026 \pm 0.0005$.²⁰ We believe that the g factor of this salt is determined by the g tensor of the TCNQ radical anion. The EPR line width shows strong angular dependence and varies in b^*a^* and cb^* planes from 0.1 to 3 mT. In summary, at room temperature the crystal exhibits weak g -factor anisotropy and strong line width anisotropy.²¹

EPR spectra were recorded from room temperature down to 140 K. With decreasing temperature the amplitude of the line decreased, and below 140 K the signal became too weak to be analyzed properly. Upon cooling, at 245 K, the EPR single line splits into three lines: the relatively broad central one and two narrow lines. Such a spectrum is typical for TCNQ salts.²²⁻²⁴ Two narrow lines are ascribed to thermally activated triplet spin excitons (TSE). Figure 5 presents representative EPR spectra at room temperature and at 170 K.

Figure 6 presents the angular dependence of the triplet-state spectra. The measurements were done at $T = 170$ K, where the amplitude of the signals was the largest. The experimental triplet-state spectra can be described by the following spin Hamiltonian:

$$\tilde{H} = \beta B g S = S \hat{D} S$$

where the first part describes the Zeeman interaction and the second one the exchange interaction between the spins. The exchange interaction gives the fine structure of the TCNQ spectrum. From the experimental data (Figure 6) the components of zero field splitting D and g tensors can be obtained. These parameters are presented in Table 4.

The principal axis system of both tensors coincides. The temperature affects only the value of the parameter D . The line width of the EPR of the triplet spin exciton (0.18 mT) does not exhibit any anisotropy. The central line undergoes the same angular dependence as the

(20) Jones, M. T.; Hertler, W. R. *J. Am. Chem. Soc.* **1964**, *86*, 1881.

(21) Firlej, L.; Graja, A.; Rajchel, A.; Wozniak K.; Krygowski, T. *M. Phys. Status Solidi B* **1987**, *140*, 437.

(22) Flandrois, S.; Amiell, J.; Carmona, F.; Delhaes, P. *Solid State Commun.* **1975**, *17*, 287.

(23) Hoffman, S. K.; Corvan, J. P.; Singh, P.; Sethulekshmi, C. N.; Metzger, R. M.; Hatfield, W. E. *J. Am. Chem. Soc.* **1983**, *105*, 4608.

(24) Hams, R. H.; Keller, H. J.; Nöthe, D.; Werner, M. *Mol. Cryst. Liq. Cryst.* **1981**, *65*, 179.

(19) Wertz J. E.; Bolton, J. R. *Electron Spin Resonance*; Chapman and Hall: New York, 1986.

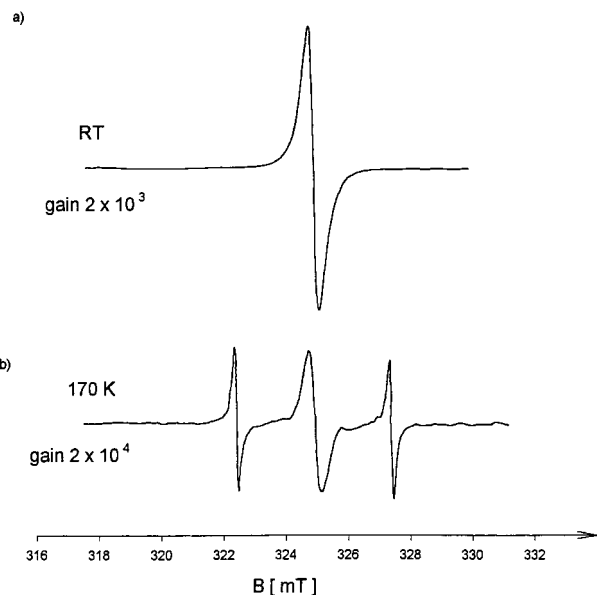


Figure 5. EPR spectrum of the complex **2a**·(TCNQ)₃ (a) at room temperature and (b) at 170 K.

triplet lines. Additionally, the linewidth of the central line is strongly anisotropic changing from 0.3 to 1 mT at $T = 170$ K. Hence this line is most likely due to the isolated anion–radical TCNQ.

The EPR technique gives a direct measurement of the spin susceptibility. The susceptibility for a Lorentzian EPR line was estimated using the formula

$$\chi \sim (\Delta B_{pp})^2 I_{max}$$

where ΔB_{pp} is the peak-to-peak line width of the first derivative signal and I_{max} is the amplitude of EPR line. The temperature dependence of spin susceptibility is described by the singlet–triplet expression:

$$\chi(T) = C/T[3 + \exp(-J/kT)]^{-1}$$

where C is Curie constant and J is the exchange constant. The fit of experimental data to this equation gives $J = 0.15$ eV for DTDAF·(TCNQ)₃. Because there is no uniform charge distribution on TCNQ molecules, there is no simple interpretation of the exchange constant J .

Electrical conductivity has been measured with the four-point method in the long axis direction of the single crystal. For the direction perpendicular to the long axis of the crystal the two-point method was applied. At room-temperature, the long c axis conductivity has attained the value of about 1.3×10^{-3} S/cm while in the perpendicular direction it is equal to 1.25×10^{-2} S/cm. Preliminary analysis of the temperature dependence of conductivity suggests that electrical transport along c axis of the crystal can be described by the variable-range hopping model, while in the perpendicular direction the model of a band semiconductor with a constant energy gap of $\Delta E = 0.29$ eV can be applied.

Conclusion

In conclusion, we have prepared DTDAF showing high electron-donating properties and demonstrated that the in situ approach can be used for the generation

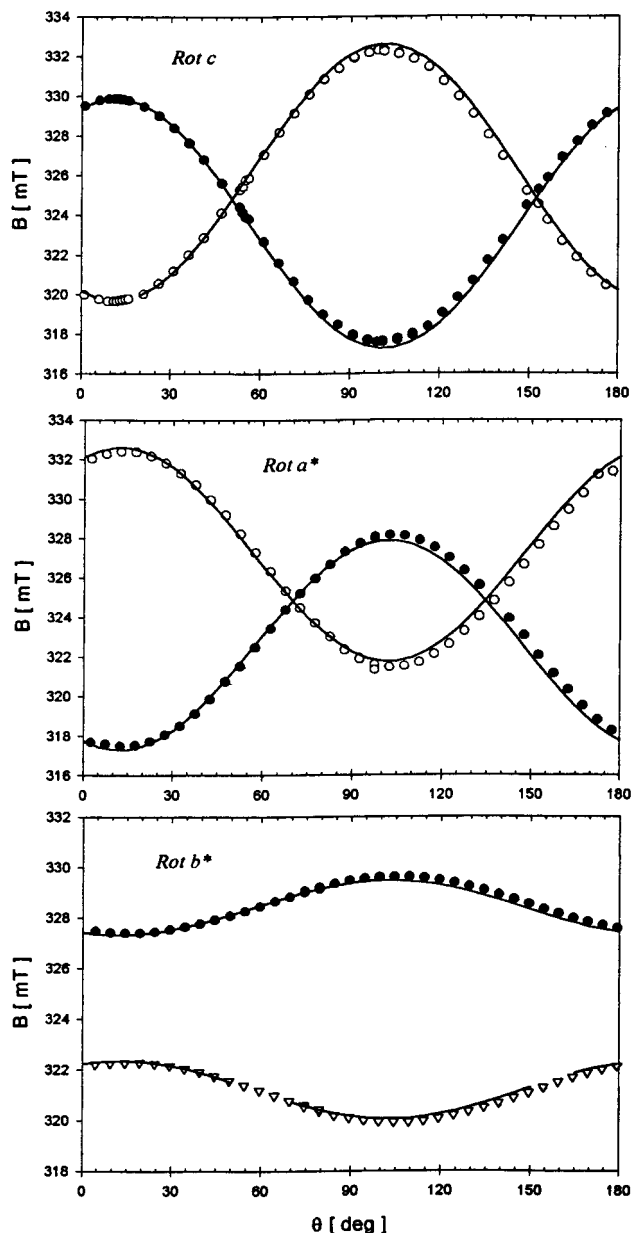


Figure 6. Anisotropy of triplet spin exciton (TSE) lines at $T = 170$ K in three mutually perpendicular planes. The solid lines are the result of fitting the data to the spin Hamiltonian.

Table 4. Directional Cosines of Principal Axes System of g^2 and D Tensors Relative to EPR Coordinate System a^* , b^* , and c and Principal Values of D and g^2 Tensors at $T = 170$ K

axes	directional cosines			g	D (cm ⁻¹)	E (cm ⁻¹)
	a^*	b^*	c			
D_{xx}	-0.3692	0.1133	-0.9224	2.0028	0.0113	0.0026
D_{yy}	-0.9117	-0.2370	0.3357	2.0034		
D_{zz}	-0.1806	0.9649	0.1908	2.0023		
	av g			2.0028		

of a DTDAF–TCNQ complex. According to the redox potential of the TCNQ, this acceptor easily oxidized the hexamethyl DTDAF to the dication, which has been proved by structural and EPR studies. Important conformational modifications between the neutral state and

(25) Bryce, M. R.; Moore, A. J.; Hasan, M.; Ashwell, G. J.; Fraser, A. T.; Clegg, W.; Hursthouse, M. B.; Karaulov, A. I. *Angew. Chem., Int. Ed. Engl.* **1990**, 29, 1450.

the dicationic one have been found. This dication functions as a counterion rather than participating in the π -electron conduction.²⁵

Experimental Section

¹H NMR spectra were recorded at 300 MHz and ¹³C NMR spectra at 75 MHz with CDCl₃ as solvent and tetramethylsilane as internal reference. Mass spectra were carried out at Centre de Mesures Physiques de l'Ouest, Rennes. Elemental analysis results were obtained from the Laboratoire Central de Microanalyse du CNRS (Lyon).

Dithiocarbamate Salt 3. Methylamine (20 mL of a 40% solution in water) was first extracted with Et₂O (3 × 50 mL) and dried over MgSO₄, and then to the solution were added 6.7 mL of triethylamine (48 mmol) and 60 mL of carbon disulfide. The mixture was stirred for 2 h at room temperature. The precipitate, white powder, was filtered, washed with Et₂O, dried under vacuum, and used without further purification. (5.5 g, yield 82%), mp 115 °C. ¹H NMR (D₂O): δ 1.17 (t, 9H, CH₃, ³J = 7.3 Hz), 2.89 (s, 3H, CH₃), 3.10 (q, 6H, CH₂, ³J = 7.3 Hz). ¹³C NMR (D₂O): δ 11.06, 37.12, 49.38, 213.58.

1,3-Thiazoline-2-thione (4). Dithiocarbamate salt (5.5 g, 2.6×10^{-2} mol) was dissolved in 100 mL of acetonitrile and the α -halogenated ketone R¹COCHXR² (2.6×10^{-2} mol) was added dropwise. The reaction mixture was stirred at room temperature for 5 h. The solvent was removed and sulfuric acid 98% (2.5 mL) was added to the resulting oil. After 15 min of stirring, water (50 mL) was added and the reaction mixture was extracted with CH₂Cl₂ (2 × 100 mL). The organic phase was washed with water (3 × 100 mL), dried over MgSO₄, and evaporated. The residue was chromatographed on silica gel column with CH₂Cl₂ as eluent and afforded thiazoline thione, which was recrystallized from EtOH.

4a: R¹ = CH₃, R² = CH₃, white powder, yield 78%, mp 98–99 °C. ¹H NMR (CDCl₃): δ 2.10 (s, 3H, CH₃), 2.13 (s, 3H, CH₃), 3.58 (s, 3H, CH₃). ¹³C NMR (CDCl₃): δ 12.09, 13.53, 35.36, 117.74, 135.19, 185.85. Anal. Calcd for C₆H₉NS₂: C, 45.25; H, 5.70; N, 8.79; S, 40.26. Found: C, 45.37; H, 5.70; N, 8.83; S, 40.03.

4b: R¹ = CH₃, R² = H, white powder, yield 80%, mp 112 °C. ¹H NMR (CDCl₃): δ 2.21 (s, 3H, CH₃), 3.55 (s, 3H, CH₃), 6.23 (s, 1H, =CH). ¹³C NMR (CDCl₃): δ 16.15, 34.63, 106.40, 140.37, 188.29. Anal. Calcd for C₅H₇NS₂: C, 41.35; H, 4.86; N, 9.64; S, 44.15. Found: C, 41.52; H, 4.79; N, 9.69; S, 44.19.

4c: R¹ = H, R² = H, white powder, yield 61%, mp 45 °C. RMN ¹H NMR (CDCl₃): δ 3.63 (s, 3H, CH₃), 6.58 (d, 1H, =CH, ³J = 4.5 Hz), 7.05 (d, 1H, =CH, ³J = 4.5 Hz). ¹³C NMR (CDCl₃): δ 38.00, 111.40, 132.86, 187.91. Anal. Calcd for C₄H₅NS₂: C, 36.62; H, 3.84; N, 10.67; S, 48.87. Found: C, 39.94; H, 3.84; N, 10.76; S, 48.70.

4d: R¹ = CH₃, R² = COCH₃, white powder, yield 90%, mp 123 °C. ¹H NMR (CDCl₃): δ 2.31 (s, 3H, CH₃), 2.61 (s, 3H, CH₃), 3.62 (s, 3H, CH₃). ¹³C NMR (CDCl₃): δ 16.28, 30.84, 35.00, 120.73, 147.56, 188.19, 188.62. Anal. Calcd for C₇H₉NOS: C, 44.90; H, 4.84; N, 7.48; S, 34.24. Found: C, 44.93; H, 4.78; N, 7.46; S, 34.10.

1,3-Thiazoline Selone 6. To a solution of thione **4** (1.5 mmol) in CHCl₃ (20 mL) was added HC(OEt)₃ (2 mL, 12 mmol) and Et₂O·BF₃ (2 mL, 16 mmol). The reaction mixture was refluxed for 20 min and stirred at room temperature for 12 h. Dry ether (25 mL) was added to the solution, the resulting oil was washed several times with Et₂O, **5** as an oil was dried under vacuum and used for cyclic voltammetry experiments without further purification. A solution of **5** in dry CH₃CN (20 mL) was slowly added to a mixture of NaBH₄ (2.2 mmol) and selenium powder (2 mmol) in degassed absolute ethanol (50 mL). After stirring for 30 min, the reaction mixture was poured in a 2% acetic acid solution (50 mL). The red precipitate was filtered off and washed with CH₂Cl₂ several times. The aqueous layer was separated from the filtrate and extracted with CH₂Cl₂. The combined organic phases were washed with water (3 × 100 mL) and dried over MgSO₄, and the solvent was evaporated. The residue was dissolved in

toluene washed with water and dried over MgSO₄, and the toluene was removed under vacuo. The residue was chromatographed on silica gel column with CH₂Cl₂ as eluent, recrystallization from EtOH afforded thiazoline selone **6**.

6a: R¹ = CH₃, R² = CH₃, white powder, yield 95%, mp 114 °C. RMN ¹H NMR (CDCl₃): δ 2.11 (s, 3H, CH₃), 2.20 (s, 3H, CH₃), 3.70 (s, 3H, CH₃). ¹³C NMR (CDCl₃): δ 12.31, 13.81, 38.03, 122.51, 137.44, 177.93. Anal. Calcd for C₆H₉NSSe: C, 34.96; H, 4.40; N, 6.79. Found: C, 34.70; H, 4.39; N, 6.77.

6b: R¹ = CH₃, R² = H, white powder, yield 65%, mp 127 °C. ¹H NMR (CDCl₃): δ 2.34 (d, 3H, CH₃, ⁴J = 1.0 Hz), 3.74 (s, 3H, CH₃), 6.53 (q, 1H, =CH, ⁴J = 1.0 Hz). ¹³C NMR (CDCl₃): δ 16.14, 37.19, 111.03, 142.48, 180.91. Anal. Calcd for C₅H₇NSSe: C, 31.26; H, 3.67; N, 7.29. Found: C, 31.14; H, 3.68; N, 7.24.

6c: R¹ = H, R² = H, yellow powder, yield 74%, mp 69–70 °C. ¹H NMR (CDCl₃): δ 3.75 (s, 3H, CH₃), 6.84 (d, 1H, =CH, ³J = 4.4 Hz), 7.22 (d, 1H, =CH, ³J = 4.4 Hz). ¹³C NMR (CDCl₃): δ 40.62, 116.05, 134.91, 180.50. Anal. Calcd for C₄H₅NSSe: C, 26.97; H, 2.83; N, 7.86. Found: C, 27.24; H, 2.88; N, 7.96.

6d: R¹ = CH₃, R² = COCH₃, orange powder, yield 43%, mp 107 °C. ¹H NMR (CDCl₃): δ 2.36 (s, 3H, CH₃), 2.71 (s, 3H, CH₃), 3.76 (s, 3H, CH₃). ¹³C NMR (CDCl₃): δ 15.67, 30.86, 37.64, 125.03, 148.61, 182.83, 188.34. Anal. Calcd for C₇H₉NOSSe: C, 35.90; H, 3.87; N, 5.98. Found: C, 36.10; H, 3.92; N, 5.94.

2a·(TCNQ)₃. To a solution of thiazoline selone **6a** (10 mg, 4.85×10^{-2} mmol) in degassed toluene (2 mL) was added freshly distilled P(OEt)₃ (8 μ L, 5.92×10^{-2} mmol). The reaction mixture was heated to 110 °C under argon for 30 min. After cooling to room temperature, a solution of TCNQ (40 mg, 0.195 mmol) in degassed CH₃CN (3 mL) was added very slowly. After 3 days black shiny single crystals were filtered off and washed with toluene.

Cyclic Voltammetry. They were carried out on a 10^{−3} M solution of thiazolium salt **5** in acetonitrile, containing a 1 M tetrabutylammonium hexafluorophosphate as the supporting electrolyte. Voltammograms were recorded at 0.1 V s^{−1} at a platinum disk electrode ($A = 1$ mm²).

X-ray Measurements. A black platelike crystal was mounted on a STOE IPDS single φ axis diffractometer with a 2D area detector based on Imaging Plate technology (graphite-monochromated Mo K α radiation, $\lambda = 0.71073$ Å). Crystal data: C₁₂H₈N₂S₂·(C₁₂H₄N₄)₃; $M = 866.98$; triclinic; space group P1 (no. 1); $a = 7.9178(9)$, $b = 9.9959(11)$, $c = 13.883(2)$ Å; $\alpha = 88.046(12)$, $\beta = 79.905(12)$, $\gamma = 86.851(11)^\circ$; $V = 1079.8(2)$ Å³ (from 2000 reflections, $3 \leq 2\theta \leq 50^\circ$); $Z = 1$; $D_c = 1.333$ g cm^{−3}; $F(000) = 448$; $\mu = 1.77$ cm^{−1}. Data collection: 130 images were recorded at room temperature by using the rotation method ($0 < \varphi < 260^\circ$) with $\Delta\varphi = 1.5^\circ$ increments, an exposure time of 1.5 min, and a crystal to plate distance of 80 mm. The images were recorded and processed with the set of programs from STOE^{12a} (EXPOSE, DISPLAY, INDEX, CELL, PROFILE, INTEGRATE, FACEIT), $2\theta \leq 50^\circ$, 8803 total data, 6192 unique data ($R_{\text{int}} = 0.0461$) of which 5333 are observed ($I \geq 2\sigma(I)$), numerical absorption correction. The structure was solved by direct methods (SHELXS-86)^{12b} and refined by full matrix least-squares calculations (SHELXL-93),^{12c} against F^2 of all data (non-H atoms with anisotropic displacement parameters, all H located in a difference Fourier map but introduced at calculated positions (riding model) in the final stage of refinement), total of 578 parameters. Convergence for observed data (for all data) at $R(F) = 0.0399$ (0.0477); $wR(F^2) = 0.0952$ (0.0982); goodness-of-fit 0.991; residual $\Delta\rho_{\text{max}} = 0.19$; $\Delta\rho_{\text{min}} = -0.21$ e Å^{−3}.

Full crystallographic details, excluding structure factors, have been deposited at the Cambridge Data Centre (CCDC). Any request to the CCDC for this material should quote the full literature citation and the reference number CCDC 118538.

EPR studies on single crystal of DTDAF(TCNQ)₃ were recorded on RADIOPAN SE/X-2547 spectrometer with TM₁₀₂

cavity and 100 kHz magnetic modulation. The spectrometer was equipped with a flowing helium Oxford ESR cryostat and temperature control unit.

Acknowledgment. We thank Dr. M. Augustyniak for orienting the crystal and Professor P. B. Sczaniecki

and Dr. W. Kempinski for assistance in performing EPR measurement.

Supporting Information Available: Temperature dependence of electrical conductivity. This material is available free of charge via the Internet at <http://pubs.acs.org>.

CM990233T